Effects of Injection Pressure and Ambient Temperature on Spray Characteristics of Water Emulsified Diesel

Ming Huo[1], Shen-lun Lin[2], Karthik Nithyanandan[1], Haifeng Liu[3], Chia-fon F. Lee[1, 4*]
[1]Department of Mechanical Science and Engineering
University of Illinois at Urbana-Champaign
Champaign, IL 61801 USA
[2] Department of Environmental Engineering
National Cheng Kung University
Tainan 70101 Taiwan
[3]State Key Laboratory of Engines
Tianjin University
Tianjin 300072 China
[4]Center for Combustion Energy and State Key Laboratory of Automotive Safety and Energy
Tsinghua University
Beijing 100084 China

Abstract

The effects of injection pressure and ambient temperature on spray characteristics of water emulsified diesel were investigated in a constant volume combustion chamber. The bubbles' size of the water phase in the fuel was first measured using a microscope for all the prepared fuels and stability tests were conducted to ensure no phase separation occurred before measurement. The fuels were later injected and combusted in a constant volume chamber with optical access. The evolution of the entire injection was record by a high speed camera using Mie scattering. The images were processed to acquire the spray characteristics such as liquid penetration and cone angle; and as such, the impacts of the ambient temperature and injection pressure on the spray performance were evaluated. It is shown that both W10 (10% water by volume) and W20 were characterized by longer liquid penetration, especially under low ambient temperatures, which was attributed to the low volatility of the water. Noticeably increased cone angles and "fattened" main jet body were observed for emulsified fuel at the beginning stage of injection indicating the possible occurrence of micro-explosion.

Key words**:** Water emulsified diesel, micro-explosion

[*]Corresponding author: cflee@illinois.edu

Introduction

The stringent emission regulations as well as the limited available petroleum resources around the world are driving both the automotive manufacturers and academia to find new technologies for cleaner and more efficient combustion in the internal combustion engine. One promising method is to use emulsified fuel, which can economically solve the classic diesel engine dilemma known as the "Particulate Matter (PM)-NO_x trade-off", since a reduction of both exhaust emissions has been found by using water-in-diesel fuels in direct injected compression ignition engines [1-5]. The emulsified fuel's capability of reducing the NO_x can be attributed to the vaporization of water, which lowers the flame temperature and thus notably reduces the NO_x emission. As for the soot reduction, it can be explained by the better air fuel mixing process featured by the enhanced atomization since micro-explosion may occur due to the drastic volatility difference between the different phases of the fuel, moreover, the water dissociation can form hydroxyl radicals during combustion which help to oxidize the soot thus reducing the soot emission [6].

Although emulsified fuel is considered an environmentally preferable alternative with tremendous emission reduction potential to be incorporated into the current fleet of diesel engines without major engine modifications, there remain several issues among which the stability should probably be most important [7-9]. Ghannam [9] reported that the surfactant is crucial to stabilize the emulsion; 0.2% surfactant and 2 minutes mixing time can stabilize 10% and 20% emulsified diesel for up to 4 weeks and 10 days respectively, however, with water content higher than 20%, the stability period is limited to 5 hours even after increasing the surfactant concentration. The ignition delay of the emulsified fuel combustion is another issue as the ignition delay time will increase greatly with the presence of water. Ghojel et al. [10] has found that the ignition delay for the diesel-water emulsion is always longer than that of the diesel fuel. Whereas the injection pressure has little impact on the ignition delay, the ambient temperature could significantly influence the ignition delay especially at higher water content, thus injection modification might be required to maintain the engine performance. The current study will address these issues by exploring the impact of hydrophilic-lipophilic-balance value (HLB) on the stability of the emulsified fuels and by evaluating the impact on ambient conditions on the ignition delay.

The other aim of this study is to investigate the micro explosion phenomena in a spray flame. The micro explosion, associated with enhanced atomization and better fuel/air mixing, has always been considered one of the major reasons for emission reduction by using emulsified fuel. Although numerous researchers have shown the existence of micro-explosion for a single fuel droplet [11-13], the presence of such phenomena in the spray injected by a regular diesel injector is still open for debate. The discovery of micro-explosions in droplet combustion arouses interest of researchers in finding similar evidence in real engine combustion. The presence of micro-explosion in atomized emulsion sprays were demonstrated in separate experiments by a number of investigators [14-17]. The direct flame photographs, temperature profiles and micro-explosion frequencies have been shown by Fuchihata et al [14]. They reported observation of small droplets whose diameter were less than 50 μm exploding in the spray flame. Wu et al [16] used the laser holography shadowgraph to visualize the spray in a diesel/water/ethanol emulsion in which an apparent raised part can be seen in the main jet body and claimed as the evidence of the micro-explosion. In a recent study of Raul et al. [17], "glowing spots" have been reported and might have resulted from micro-explosion. It should be noted that there remain substantial differences between the single droplet and fuel jet experiment. The velocities of the droplets in a reacting spray jet can reach up to ~100 m/s while the fuel droplet is quiescent in the single droplet combustion; the primary and secondary breakup due to the high jet momentum and aerodynamic force may also affect the occurrence of micro-explosion. Therefore, the speculation that micro-explosions can occur in spray combustion needs to be supported by experimental evidence derived from spray studies. It is also interesting to discover the injection and ambient conditions that favor the occurrence of micro explosion.

Experimental Methods

Preparation of emulsified fuel

An ultra low sulfur diesel (ULSD) obtained from Illini FS was used as a base fuel and the oil phase in emulsified diesel in current study. The cetane index, 90% distillation point, total sulfur, flashpoint, and viscosity of the base fuel regulated by American Society for Testing and Materials (ASTM) are tabulated in Table 1. In a previous study [7], the three phase oil-in-water-in-oil (O/W/O) emulsions were reported more stable than two phase water-in-oil (W/O) emulsion. Thus a two-step procedure was utilized to prepare the O/W/O emulsions in this research. A hydrophilic surfactant polyoxyethylene sorbitan monooleate (TWEEN 80) with HLB = 15 was added into water for reducing the interfacial tension and retarding the flocculation, coalescence, and creaming between oil and water phases. On the other hand, the lipophilic surfactant Sorbitan oleate (Span 80) with HLB = 4.3 was added into ULSD to stabilize the oil phase. A

magnetic stirrer (Temper, Fisher Scientific Inc.) was employed to mix and heat the water and ULSD while the TWEEN 80 and Span 80 were added in respectively.

An O/W emulsion was first prepared by adding 1/9 in volume USLD into water-TWEEN 80 mixture and blended at 10000 rpm for 5 minutes. The above emulsion was then gently poured into the specific amount of ULSD-Span 80 mixture and emulsified for a period of time at 50 °C and 10000 rpm to form O/W/O emulsion. The blending time period, including 5, 10, 20, 30 minutes, were optimized by the later stability tests. In addition, the HLB value is the most referable parameter of surfactant selection and addition in emulsification process while the higher HLB stands for more hydrophilic tendency of a surfactant. Emulsions of different HLB values were prepared by Span 80 and TWEEN 80 while the combined HLBs were calculated by the following equation:

$$HLB_{\mathrm{Pool}} = HLB_{\mathrm{S}} * \mathrm{W_S} + HLB_T * W_T \quad (1)$$

where the suffixes S and T stands for Span 80 and TWEEN 80 respectively; W represents the mass ratio of each surfactant ($W_S + W_T = 1$). In the current study, the tested HLB ranged from 5.0~8.0 to prepare 700 mL O/W/O emulsion while the optimization of HLB value took place by stabilizing 20 vol. % water in a O/W/O emulsion and were tested in terms of their stability. The water contents varied from 5 to 20 vol. % in this study with the fixed 2 vol.% total surfactant ratio.

Molecular formula	C_{12}-C_{25}
Cetane index	40 (min.)
Total sulfur (ppm)	7~15
Density (g/ml)	0.82-0.86
Auto-ignition temperature (°C)	~210
Lower heating value (MJ/kg)	42.5
Flash point (°C)	65-88
Boiling point (°C)	180-230
90% distillation point (°C)	293.3~332.2
Viscosity (cst)	1.5~4.5

Table 1. Base line fuel properties

Fuel stability tests

There were three parameters to be optimized by emulsion stability tests, including blending duration, HLB values, and water contents. The following two methods were employed to characterize the stability of the emulsion: (1) a two-week (14-day) continuous record of fuel daily changes; and (2) observation and analysis of W/O droplet sizes using an optical microscope (OLYMPUS BX51TF, TOKYO, JAPAN) with 400x amplification and a charge-coupled device (CCD) video camera (OLYMPUS DP20). The first method observed the destabilization of emulsion after the short term storage. 15 mL of each tested fuel was stored in a centrifugal tube at 25°C right after it's production. The higher separated volume at the bottom of tube after 14-day standing indicates lesser stability of emulsion. In order to estimate the fuel condition after a long-term storage, the second method was used to capture the image and calculate the Sauter mean diameter (SMD) of O/W/O bubbles by using the Image-Pro Plus software version 5.0.2.9. By the bubble size distribution and SMD measurement, the tendency of phase separation could be described while the 14-day test showed no separate layer.

Experimental Setup and Procedure

A constant volume chamber with a bore of 110 mm and a height of 65 mm is used in this study. The chamber can imitate the spray and combustion process of a diesel engine, allowing a maximum operating pressure of 18 MPa. The chamber has an open end on the top with a fused silica (Dynasil 1100) end window installed opposite to the injector, allowing optical access. The fused silica end window, sealed by a Tamshell energized spring seal, is 130 mm in diameter and 60 mm in thickness, with a high UV transmittance down to 190 nm. A six-hole Caterpillar hydraulic-actuated electronic-controlled unit injector (HEUI) is mounted at the center of the chamber head. Four injection pressures ranging from 70 MPa to 130 MPa were used in this study. The cylinder wall is heated to 380 K by eight heaters (Watlow Firerod), to mimic the wall temperature of a diesel engine as well as to prevent water condensation on the optical windows. Nevertheless, the oil line and fuel line inside the chamber head are kept at 350 K to simulate the situation in an actual engine and stop the fuel evaporation before injection. A Kistler 6121 quartz pressure transducer is embedded in the chamber wall in conjunction with a 5026 dual mode differential charge amplifier. All pressure data and were ensemble averaged over at least eight injection events, and the apparent heat release rate (AHRR) data were calculated from filtered, averaged pressure data using an air-standard first-law analysis.

The procedure is started by filling the chamber to a specified density with a premixed, combustible-gas mixture, including acetylene (C_2H_2), 50/50 oxygen and nitrogen, and air as shown in Fig. 1a. The mixture is pushed into the chamber by a piston accumulator and then ignited with a spark plug. By burning the mixture, a high-temperature, high-pressure environment in the chamber is created. Acetylene, with unity C/H ratio, is

used as the combustible gas for its flammability and low window contamination. Equation (2) shows the chemical reaction of the mixture,

$$4\ \ C2H2 + (10 + \zeta)O2 + 65\,N2 \rightarrow 8\,CO2 + 4\,H2O + \zeta\,O2 + 65\,N2 \quad (2)$$

where ζ denotes the amount of excess oxygen. The chamber ambient contains 21% oxygen, 66.7% nitrogen, 8.2% carbon dioxide and 4.1% water vapor by volume after burning the mixture. The molecular weight for the post-combustion gas mixture is 29.738 kg/kmole, and the density is 14.8 kg/m^3. As the products of combustion cool over a relatively long time (~2 s) due to heat transfer to the vessel walls, the vessel pressure slowly decreases. When the desired experimental conditions are reached, the HEUI injector is triggered and the fuel injection, auto-ignition and combustion processes ensue. The ambient gas temperature, density, and composition at injection are determined by the pressure at the time of fuel injection and the initial mass and composition of gas within the chamber. For the experiments presented in this paper, three different ambient temperatures were considered: 800, 1000 and 1200 K, covering both low-temperature combustion and conventional combustion in diesel engine.

Image Processing

High speed images for both spray and combustion studies are obtained with a non-intensified high speed digital camera (Phantom V7.1), located above the optical chamber. For the spray studies, the light source is supplied by a copper vapor laser (Oxford Lasers LS20-50) which can be externally controlled to run up to a maximum frequency of 50 kHz with pulse duration of 25 ns. The high-speed camera and the copper-vapor laser were synchronized up to 15,037 frames per second to produce time resolved measurement at a spatial resolution of 512×256 pixels. A Nikkor 105 mm focal length lens was used for the high-speed imaging and an exposure time of 3 μs was used. The copper-vapor laser has two-color output, at 511 and 578 nm, with a power ratio of 2:1. To filter out the light at 578 nm for this monochromatic light extinction, two interference filters at 510 nm and 515 nm with 10 nm full width at half maximum (FWHM) achieving a 5 nm FWHM were used. The interference filters also served to block the visible soot luminosities, though the intensive soot emission, especially at high ambient temperature cases, may still contribute to the signal gain and raise noises in the determination of the liquid penetration. The scattered light emitted from the fiber was condensed by an aspheric condenser lens and then reflected via a mirror of 6 mm diameter placed in front of the condenser lens that could be considered as from a point source before entering the chamber. A schematic drawing of the setup is shown in Fig. 1b. The camera was triggered to start the recording by the injection signal and was set to record for a duration long enough to cover the entire duration of spray and combustion. The spatial resolution of the camera was typically 0.108 mm/pixel.

Shadowgraphs based on the diffraction index variation for vapor-air localization has been used for quite a long time. The use of this technique, usually involving two optical windows installed inline on a test chamber, was motivated against elastic scattering because of the difficulties involved in discriminating the border between the vaporized fuel and surrounding air in reacting environments as pointed out by a few researchers [17,18]. In the present study, a similar principle based on the reflection index variation instead of diffraction index variation has been adopted since only one optical accessible window is installed on the top of the chamber. The raw images obtained from each complete injection sequence were first corrected by the first image of the respective sequence which was taken right before the fuel injection. The histogram equalization was then performed to enhance the contrast of each image and minimized the effect of the illumination intensity variation due to the ambient temperature difference and light degradation from case to case. It is also found that this procedure eliminate the bulk noise of the background which later makes easier the determination of both the liquid penetration and cone angle. As the camera will capture stronger reflection signal of the laser beam from the spray, the liquid penetration length can be defined as the distance between the injector tip and the first pixel above a preset threshold along the jet centerline. The determination of the threshold has been discussed by a number studies. In a recent study of Raul et al. [17], both the centerline intensities and the derivatives have been used to divide the spray jet into continuous liquid core, droplets and fuel vapors. After performing a similar analysis, the author found the determination of the droplets penetration and vapors penetration could be very challenging and subjected to inconsistency due to the aforementioned soot luminosity noise in the background as can be seen in Fig. 2. Therefore, only one threshold was chosen in the present study and was referred to as the liquid penetration. It is also worthwhile to mention that penetration is not merely decided by "one" pixel touching the threshold, but rather a 3×3 pixel arrays whose value are all above the threshold, such that the impact of the noise can be minimized. Once the liquid penetration was determined, the cone angle can be measured by finding the farthest 3×3 pixel array above the same preset

threshold perpendicular to the jet centerline in a similar fashion as the liquid penetration determination. All the quantitative results were ensemble averaged over at least eight injection events.

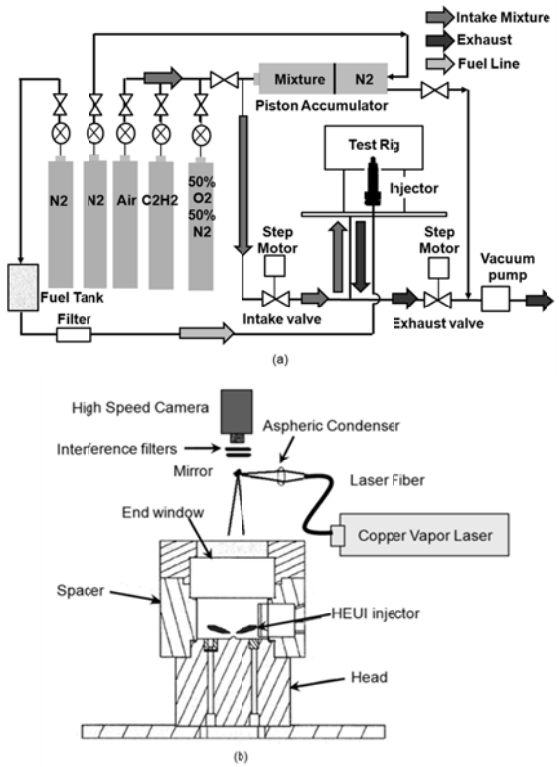

Figure 1. (a) Schematic of the experimental setup; (b) Schematic of test rig

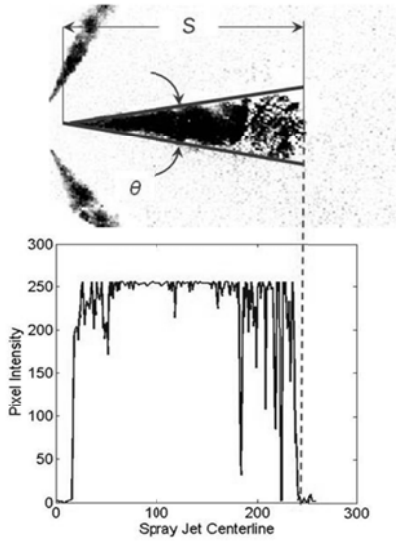

Figure 2. Determination of the liquid penetration

Results and Discussion

Fuel stability

After a 14-day standing period, separate layers occurred in the tubes of HLB equal to 6, 7, and 8, which were 8, 16, and 20% volume of total emulsion, respectively. Therefore, nearly no separate layer, milky white liquid of emulsion indicated that the HLB = 5 is the relatively suitable surfactant composition to the diesel/water interfacial condition. However, both blending duration time and water content did not show any significant effect in the appearance of emulsion and because of that all the O/W/O diesel with different water contents and operation times stayed in a stable, one, crystalline phase. Thus, the more micro-scale observation becomes important.

The bubble size distribution and SMD could also grade the homogeneities of different fuels. The smaller droplet diameter leads to the greater reaction surface per volume of fuel, thus promoting more complete combustion. Fig. 3 showed the bubble appearances, sizes and homogeneities of the 5, 10, 15, and 20 vol. % water-containing emulsified fuels under a 400x microscope. Obviously, the 5 vol. % water emulsified diesel (W5) had the smallest and most homogeneous bubble distribution while the big bubbles increased with increasing water content. As part of the quantitative analysis, Fig. 4 shows the probability density function (PDF) of the O/W/O bubble sizes. The PDF curves displayed the W5 and W10 had relatively higher fractions of small bubbles around 2 μm while W15 and W20 had lower peak values at the smaller diameter region. Additionally, all of the W10, W15 and W20 had an extra peak close to 4 μm of diameter which means more non-homogeneous distribution than W5. The volumetric density function (VDF) in Fig. 5 was defined as:

$$\text{VDF}=\frac{\text{the volume ratio (vol.\%) of (bubble with specific diameter)}}{\text{(overall bubble volume)}} \quad (3)$$

VDF could amplify the contribution of those huge bubbles with small number, which could not be shown in PDF graph. According to the VDF, the specific bubbles with relatively longer diameter were found around 17~21 μm and 24~30 μm in W15 and W20 curves, respectively. The above results reveal that the destabilizing tendency increased with the increasing water content; even W20 still stay as a stable milky emulsion after 14-day standing.

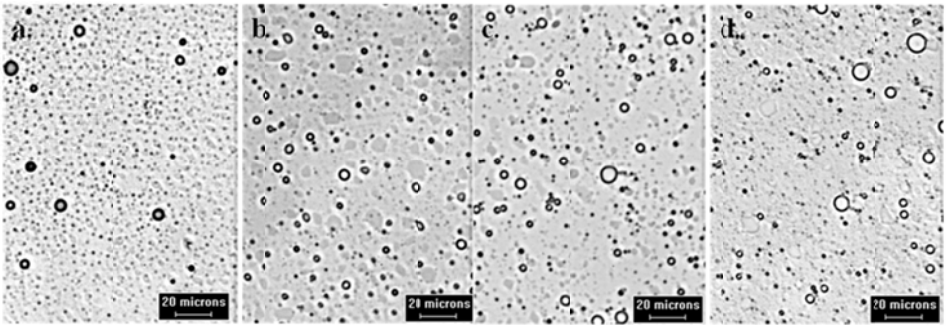

Figure 3. O/W/O bubbles of water-diesel emulsion with (a) 5%; (b) 10%; (c) 15%; and (d) 20% water contents

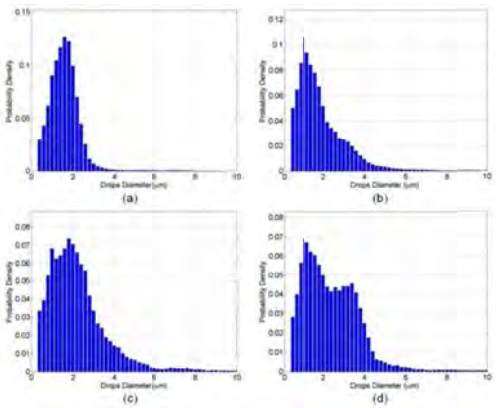

Figure 4. Probability density functions of various W/O droplet diameters (a)W5, (b)W10, (c)W15, (d)W20

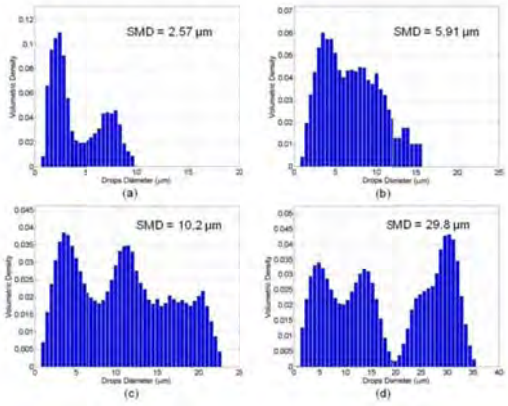

Figure 5. Volumetric densities of various W/O droplet diameters (a)W5, (b)W10, (c)W15, (d)W20

In addition, the SMD calculation showed that the extension of emulsification time did not work; the SMD of W20 with 5, 10, 20, 30 minutes operation durations were 30.2, 29.8, 30.1, and 29.8 μm, respectively. Therefore, 10 minute was practically used for its efficient and sufficient property. For grading the stability of different water additions, SMD of W5, W10, W15, and W20 were derived as 2.57, 5.91, 10.2, and 29.8 μm, respectively. This result again indicated the instability of higher water fraction in emulsion which would flocculate, coalesce, and form cream after a longer time which is supported by the aforementioned VDF graphs. However, Fu et al [18] reported that the micro-explosion strength has a maximum value around 40~60 vol. % of water and decreased in either lower or higher region. The storage energy of nucleation will be small and lead to a weak micro-explosion when the water content was small; when water ratio was large, more water was needed to evaporate and form an oil membrane, which will lead to small amount of water remaining in a dispersed bubble, nevertheless, the micro-explosion strength reduced with the increasing diameter of the dispersed bubble. Consequently, the W10 and W20 were chosen for their higher tendency and strength of micro-explosion while the storage time was restrained to two weeks in the current study.

Combustion Characteristics

The apparent heat release rates for different injection pressures and ambient temperatures, derived from the chamber pressure, are illustrated in Fig.6. It is clearly shown that among the different variables, the ambient temperature had the dominant impact on the combustion characteristics. The lower ambient temperature shifts the combustion phase towards premixed combustion, which is expected due to the longer ignition delay. The strong dependence of the ignition delay on the ambient temperature agrees with previous studies [19, 20]. It is interesting to notice that only at low ambient temperature and low injection pressure, the increase of the water content caused slightly longer ignition delay while in other cases the difference is negligible. In the study of Ghojel et al. [10], they reported an increase of both pressure ignition delay and luminous ignition of the diesel emulsion, however, with 15% water content, the ignition delay was retarded by only ~0.02 ms compared to pure diesel; once the water content reaches 35% or higher, the delay

jumps up to ~0.2 ms. This agrees with our results to some extent and confirms that with water content below 20%, the ignition delay of the emulsified diesel should not account as a major issue. The increase of the injection pressure reduced the ignition delay as the dynamics of the higher jet velocity entrained more air into the spray jet. The higher oxygen concentration in this region reduces the auto-ignition delay. The impact of the injection pressure was far less than the ambient temperature.

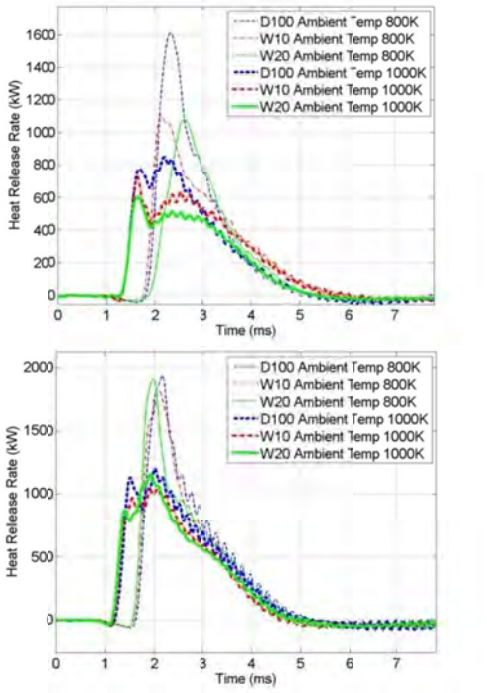

Figure 6. Apparent heat release rate at different ambient temperature (a) P_{inj}=90 MPa, (b) P_{inj}=130 MPa

Spray liquid penetration and cone angle.

The evolution of the spray for an individual cycle for the three tested fuels under different ambient temperatures with a injection pressure of 90 MPa are illustrated in Figs. 7-9 while the averaged quantitative measurement of liquid penetration and spray cone angle are shown in Fig. 10 and Fig. 11 respectively. For presentation purposes, the images presented were relatively in the beginning stages of injection and representative images were chosen to demonstrate the spray evolution for each tested fuel before it reached the "quasi-steady" state. For quantitative analysis, each curve was averaged over at least eight injection events and the shot-to-shot variation was typically within 5%.

Under low ambient temperatures, all the tested fuels presented longer liquid penetration due to the lower evaporation rate, which is consistent with previous studies [17]. Low ambient temperature provided longer fuel/air mixing time and as a consequence, more premixed burning resulted. As seen from Fig. 9, the penetration reached a peak rapidly after the injection and gradually shortened once the combustion started due to the hot gases pouring back into the spray jet together with the radiation from the soot emission, enhancing the vaporization. In comparison, the penetration under high ambient temperature were shorter and reached a quasi-steady state almost immediately after the onset of injection due to the shorter ignition delay and the rigorous diffusion flame swallowing the liquid jet spray.

Both W10 and W20 were featured with longer liquid penetration, especially under low ambient temperatures attributed to the low volatility of the water. Such variation became less apparent as the ambient temperature increased which can be explained by a few factors. The emulsified fuel has higher viscosity and surface tension than regular diesel fuel which is likely to be more resistant to shear and break up, and as the ambient temperature is elevated, both properties will decline and favor the atomization process, thus making the penetration comparable to that of pure diesel. The breakup induced by the superheating of the interior component, also known as micro-explosion could also enhance the atomization process, especially the secondary atomization [13]. It is interesting to notice that as the water content increased, W20 actually exhibited a slightly shorter liquid penetration with an injection pressure of 90 MPa, indicating the penetration is result of competition between the low volatility of water and a better atomization of the water emulsified diesel.

For all the tested fuels, the spray had a relatively larger cone angle at the very beginning of the injection and narrowed down afterwards. After around 0.4~0.8 ms, it reached a quasi-steady state though fluctuations can still be observed. Unlike the findings in the previous study [17] where the spray cone angle were monotonously decreasing, the cone angles barely exhibit any unanimous trend during the “quasi-steady” state. The fluctuation was mainly resulted from the instability along the periphery of the spray jet. The spray cone angles for water emulsified diesel were generally larger than those of diesel and the difference was more remarkable under high ambient temperature. The snapshots for a single spray, especially at the early stage (typically before 1.66ms), give more intuitive insights on the spray structure, as shown in Figs. 7-9. It can be clearly seen that some abrupt areas raised along the periphery of the spray jet body causing a "fattened" main jet body at relatively high ambient temperatures (1000K and 1200K) for the water emulsified fuel which tremendously spread the spray cone, compared to the relatively smooth spray jet and small cone angle of diesel. The raised part of the main spray jet was not

observed with the pure diesel under all circumstances, or with emulsified fuel under low ambient temperatures, indicating that its occurrence should be associated with the presence of water, or the phenomenon of micro-explosion. Under high ambient temperature, the water reached the superheating temperature more rapidly causing a shorter micro-explosion delay time. Meanwhile, each component inside the emulsified diesel was subjected to higher evaporation rate which decreased the resistance for the water bubble growth. With the combined effect, violent breakup events, manifested by the extraordinary spray shape, were taking place inside the spray jet. At lower ambient temperature, in contrast, more time is required for the water to reach super heating and more resistance for the bubble to grow up and breakthrough because of the relatively cool environment, the micro-explosion delay was significantly increased. As a result, the micro-explosion might not happen, or occur down-stream so that it won't affect the main body of the spray jet anyway.

In light of the injection pressure, it is observed that liquid penetration reached the peak value or the quasi-steady state much faster with elevated injection pressure due to the higher jet velocity. It is also observed that the liquid penetration peak increased with elevated injection pressure under low ambient temperature, though such variation was negligible at high ambient temperature indicating the smaller fuel droplet sizes induced by higher aerodynamic shear evaporated faster and compensated the longer penetration caused by the high jet velocity. The impact of the injection pressure on the spray cone angle is more pronounced, as lower injection pressure resulted in larger cone angle which is possible due to the fact that with lower jet velocity, the spray has more time to adjust to the surrounding gases and is less constrained to expand.

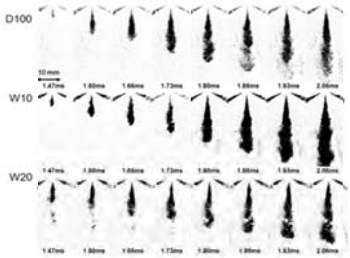

Figure 7. Spray evolution at injection pressure of 90 MPa and ambient temperature of 800K

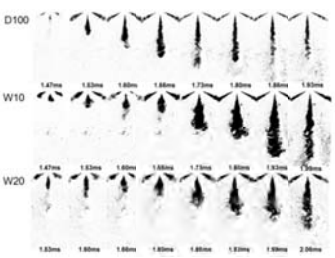

Figure 8. Spray evolution at injection pressure of 90 MPa and ambient temperature of 1000K.

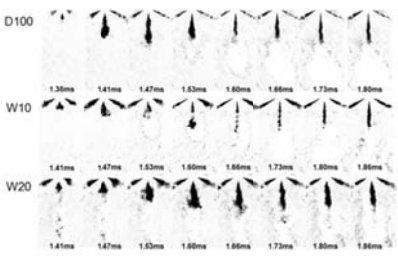

Figure 9. Spray evolution at injection pressure of 90 MPa and ambient temperature of 1200K

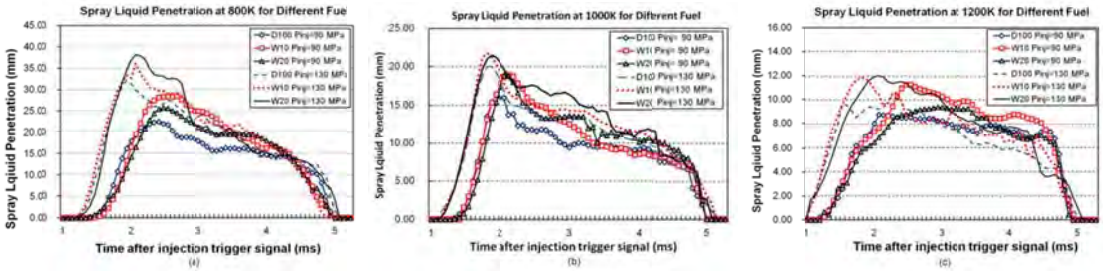

Figure 10. Liquid penetration for three tested fuels under ambient temperature of a) 800K, b) 1000K, c) 1200K

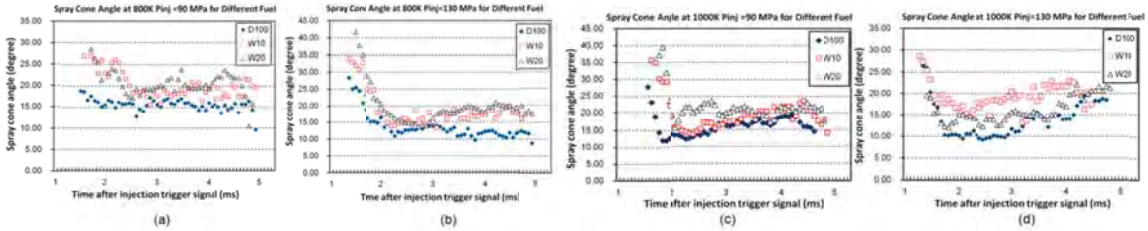

Figure 11. Spray cone angle for three tested fuels at a) T_{amb} = 800 K P_{inj} = 90 MPa, b) T_{amb} = 800 K P_{inj} = 130 MPa, c) T_{amb} =1000 K P_{inj} = 90 MPa, d) T_{amb} = 1000 K P_{inj} = 130 MPa

Summary and Conclusions

The effects of injection pressure and ambient temperature on spray characteristics of water emulsified diesel were investigated in a constant volume combustion chamber. The bubbles' size of the water phase has been measured using a microscope and stability tests have been conducted for all the prepared emulsions. All emulsified fuels tested were stable within a range of two weeks. The fuel was later injected and combusted in the constant volume chamber. A wide range of ambient conditions were applied so as to investigate their impacts on the ignition delay, spray penetration and cone angle. The findings can be summarized as follows:

1) For diesel emulsified fuels, an HLB value of 5 is relatively the suitable surfactant composition to the diesel/water interfacial condition as it stabilize the emulsion for more than two weeks, with water content reach up to 20%.

2) Ambient temperature had the dominant impact on the ignition delay compared to injection pressure and water content. With water content less than 20%, the ignition delay was only observed at the low ambient temperature together with low injection pressure, and almost negligible in all other cases indicating the ignition delay should not be considered as a major issue with low water content emulsified diesel.

3) It is shown that both W10 (10% water by volume) and W20 were characterized by longer liquid penetration, especially under low ambient temperatures, which can be attributed to the low volatility of the water. Notably increased cone angles and "fattened" main jet body were observed for emulsified fuel at the beginning stages of injection indicating the occurrence of micro-explosion.

Acknowledgements

This work was supported in part by the Department of Energy GATE Centers of Excellence Grant No. DE-FG26-05NT42622.

References

1. Valdmanis, E., and Wurlfhorst, D.E., *SAE Technical Paper* 700736 (1970).
2. Gunnerman, R.W., and Russel, R. L., *SAE Technical Paper* 972009 (1997).
3. Song, K. H., and Lee, Y. J., *SAE Technical Paper* 002794 (2000).
4. Musculus, P. P. B., Dec, J. E., Tree, D. R., Daly, D., Langer, D., Ryam, T. W., and Matheaus, A. C., *SAE Technical Paper* 033146 (2003).
5. Anna, L., Magnus, S., Savo, G., and Ingemar, D., *SAE Technical Paper* 071076 (2007).
6. Kadota, T., and Yamasaki, H., *Progress in Energy and Combustion Science* 28:385-404 (2002).
7. Lin, C. Y., and Lin, S. A., *Fuel* 86:210-217 (2007).
8. Hesampour, M., Krzyzaniak, A., and Nyström, M., *Journal of Membrane Science* 325:199-208 (2008).
9. Ghannam, M. T., and Selim, M. Y. E., *Petroleum Science and Technology* 27:396-411 (2009).
10. Ghojel, J., and Tran, X. T., *Energy and Fuels* 24:3860–3866 (2010).
11. Tsue, T., Kadota, T., and Segawa, D., *Proceedings of the Combustion Institute* 24:1629–1635 (1996).
12. Kadota, T., Tanaka, H., Segawa, D., Nakaya, S., and Yamasaki, H., *Proceedings of the Combustion Institute* 31:2125-2131 (2007).
13. Watanabe, H., Suzuki, Y., Harada, T., Matsushita, Y., Aoki, H., and Miura, T., *Energy* 35:806–813 (2010).
14. Mizutani, Y., Fuchihata, M., Matsuoka, Y., and Muraoka, M., *Transactions of Japanese Society of Mechanical Engineering* 66:1544-1549 (2000).
15. Fuchihata, M., Ida, T., and Mizutani, Y., *Transactions of Japanese Society of Mechanical Engineering* 69:1503-1508 (2003).
16. Wu, D. Y., Sheng, H. Z., Zhang, H. C., and Wei, X. L., *Journal of Xi'an Jiaotong University* 41:772-775 (2007).
17. Raul, O., Anna, L., Magnus, N., Sven, A., and Ingemar, D., *Fuel* 89:122-132 (2010).
18. Fu, W. B., Hou, L. Y., Wang, L., and Ma, F. H., *Fuel Processing Technology* 79: 107-119 (2002).
19. Sieber, D., *SAE Technical Paper* 852102 (1985).
20. Dec, J. E., and Espey, C., *SAE Technical Paper* 982685 (1998).